Bioorganic & Medicinal Chemistry 17 (2009) 3332–3341

Contents lists available at ScienceDirect

Bioorganic & Medicinal Chemistry

journal homepage: www.elsevier.com/locate/bmc

Synthesis, in vitro and computational studies of protein tyrosine phosphatase 1B inhibition of a small library of 2-arylsulfonylaminobenzothiazoles with antihyperglycemic activity

Gabriel Navarrete-Vazquez [a,*], Paolo Paoli [b,*], Ismael León-Rivera [c], Rafael Villalobos-Molina [d], Jose Luis Medina-Franco [e], Rolffy Ortiz-Andrade [a,f], Samuel Estrada-Soto [a], Guido Camici [b], Daniel Diaz-Coutiño [c], Itzell Gallardo-Ortiz [d], Karina Martinez-Mayorga [e], Hermenegilda Moreno-Díaz [a]

[a] Facultad de Farmacia, Universidad Autónoma del Estado de Morelos, Cuernavaca, Morelos 62209, Mexico
[b] Dipartimento di Scienze Biochimiche, Università degli Studi di Firenze, Firenze 50134, Italy
[c] Centro de Investigaciones Químicas, Universidad Autónoma del Estado de Morelos, Cuernavaca, Morelos 62209, Mexico
[d] Unidad de Biomedicina, FES Iztacala, Universidad Nacional Autónoma de México, Tlalnepantla, México 54090, Mexico
[e] Torrey Pines Institute for Molecular Studies, Port St. Lucie, FL 34987, USA
[f] Facultad de Química, Universidad Autónoma de Yucatán, Mérida, Yucatán 97150, Mexico

ARTICLE INFO

Article history:
Received 10 February 2009
Revised 13 March 2009
Accepted 20 March 2009
Available online 26 March 2009

Keywords:
Benzothiazoles
Protein tyrosine phosphatase (PTP-1B)
Diabetes

ABSTRACT

The 2-arylsulfonylaminobenzothiazole derivatives **1–27** were prepared using a one step reaction. The in vitro inhibitory activity of the compounds against protein tyrosine phosphatase 1B (PTP-1B) was evaluated. Compounds **4** and **16** are rapid reversible (mixed-type) inhibitors of PTP-1B with IC_{50} values in the low micromolar range. The most active compounds (**4** and **16**) were docked into the crystal structure of PTP-1B. Docking results indicate potential hydrogen bond interactions between the nitro group in both compounds and the catalytic amino acid residues Arg 221 and Ser 216. Both compounds were evaluated for their in vivo antihyperglycemic activity in a type 2 diabetes mellitus rat model, showing significant lowering of plasma glucose concentration, during the 7 h post-intragastric administration.

1. Introduction

Type 2 diabetes mellitus (T2DM) is a progressive disease of metabolic deregulation characterized by insulin resistance in peripheral tissues (liver, muscle, and adipose), and impaired insulin secretion by the pancreas.[1] Obesity is one of the major risk factors for developing T2DM.[2] Current therapies to combat both diseases are limited and often ineffective, and there is an urgent need for improved drugs that can help reverse disease progression.[3]

The enzymes protein tyrosine phosphatase PTP-1B and 11β-hydroxysteroid dehydrogenase type 1 (11β-HSD1) are both novel attractive therapeutic targets for the treatment of diabetes and obesity.[4] PTP-1B is an intracellular enzyme that has been involved in down-regulation of receptor tyrosine kinase activity following stimulation of the insulin or leptin receptors. Recently reports have demonstrated that mice lacking PTP-1B have enhanced insulin sensitivity.[5] Inhibition of PTP-1B would result in maintenance of an activated insulin receptor and hence prolong insulin signaling.

On the other hand, 11β-HSD1 catalyzes the conversion of inactive cortisone into the active hormone cortisol, which is a potent functional antagonist of insulin action, and promotes gluconeogenesis in the liver, potentially leading to raised blood glucose concentration in diabetes.[6]

Inhibition of both enzymes has been considered as attractive therapeutic targets for T2DM, obesity and metabolic syndrome.[4] Recently, our group reported a series of seven benzothiazoles related to this work, which were weak inhibitors of 11β-HSD1.[7] However, the compounds displayed appreciable in vivo activity in T2DM murine model, comparable to glibenclamide. In order to find an alternative mode of action of this class of compounds, we report in this article the one-step synthesis of an extended library of 2-arylsulfonylaminobenzothiazole derivatives, their in vitro inhibitory activity on the PTP-1B, and the in vivo antihyperglycemic effect observed with the most active compounds.

2. Results and discussion

2.1. Chemistry

The small library of title compounds (**1–27**), was designed using a matrix of four benzothiazole and six arylsulfonylchlorides. Com-

* Corresponding authors. Tel./fax: +52 777 3297089 (G.N.-V.).
E-mail addresses: gabriel_navarrete@uaem.mx (G. Navarrete-Vazquez), paolo.paoli@unifi.it (P. Paoli).

0968-0896/$ - see front matter © 2009 Elsevier Ltd. All rights reserved.
doi:10.1016/j.bmc.2009.03.042

pounds were synthesized starting from 2-aminobenzothiazole-6-substituted (**28–33**), via a coupling reaction with arylsulfonyl chlorides **34–40,** in the presence of a catalytic amount of 4-dimethylaminopyridine and triethylamine.[7] Title compounds were recovered with 26–90% yields (Table 1). Compounds were purified by recrystallization or by column chromatography. Compounds **4**, **6, 11, 16, 18** and **26** afforded the best yields; all of them contain electron-withdrawing groups attached at position four respect to the phenyl sulfonamide moiety. On the other hand, compounds **1, 13–15, 17, 19, 20**, **22** and **25**, which bear electron-donating groups at that position, had the lowest yields.

The chemical structures of the synthesized compounds were confirmed on the basis of their spectral data (NMR and mass spectra), and their purity ascertained by microanalysis. Physical constants of the title compounds are shown in Table 1.

In the nuclear magnetic resonance spectra (^{1}H NMR; δ ppm), the signals of the respective protons of the compounds were verified on the basis of their chemical shifts, multiplicities, and coupling constants. The aromatic region of the ^{1}H NMR spectrum contained an ABX pattern signals ranging from δ 6.94–6.99 (dd, *Jm* = 2.2–2.6; *Jo* = 8.8 Hz), 7.18–7.23 (d, *Jo* = 8.8 Hz), and 7.41–7.60 (d, *Jm* = 2.2–2.6 Hz) attributable to H-5, H-4, and H-7, of the benzothiazole 6-substituted structure, respectively. Compounds **6, 7, 10, 14, 21** and **23** have been previously reported.[7] Compound **3** was purified by recrystallization. A sample crystal was obtained and diffracted by X-ray analysis, confirming the proposed structure.[8]

Before the establishment of an in vitro assay, we obtained predictive values concerning biological activities by comparing the chemical structures of the compounds designed (**1–27**), with structures or substructures of more than 46,000 well-known biologically active drugs included in the database of software named Prediction of Activity Spectra for Substances (PASS).[9–12] Results presented in Table 1 describe two biological activities taken from PASS software: antiobesity and antidiabetic effects. *Pa* values estimated for antiobesity activity were ranging between 0.80 and 0.89. These results indicated that compounds exhibited chemical structures similar to known antiobesity drugs, and are likely to reveal this activity. *Pa*-estimated antidiabetic activity values were determined ranged between 0.59 and 0.72, which also indicates that chemical structures of compounds **1–27** exhibited levels of similarity to those of known antidiabetic drugs (i.e., sulfonylureas). The predictions do not include a specific target as PTP-1B or 11 β-HSD1.

2.2. In vitro biological assay

To test the ability of the compounds to inhibit PTP-1B, all compounds were dissolved in DMSO to prepare initial solutions (20 mM, final concentration), aliquots of each initial solution were diluted to 40 μM with the assay buffer containing 2 mM *p*-nitrophenyl phosphate (*p*NPP); the mixture was incubated at 37 °C, and the reaction was started by adding an appropriate enzyme aliquot.[13] The results showed that two compounds (**4** and **16**) strongly reduce the PTP-1B enzyme activity (Fig. 1). Other compounds, such as **10**, **18**, **23**, and **27**, are weaker inhibitors. It is interesting to note that all of the above compounds, with exception of **18**, bear a nitro group in their structure.

Considering the results of the preliminary PTP-1B inhibition analysis, we performed additional tests on the more potent compounds **4** and **16**. To verify if these compounds were reversible inhibitors, appropriate aliquots of PTP-1B were incubated in the

Table 1
Synthesis, physicochemical data and predictive values of biological activities calculated with PASS for derivatives **1**–**27**

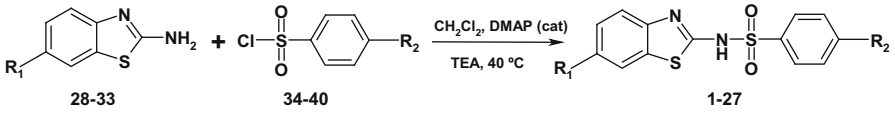

Compound	R_1	R_2	MW	Mp (°C)	Unoptimized yield (%)	Antiobesity effect (*Pa*/*Pi*)	Antidiabetic effect (*Pa*/*Pi*)
1	$-CH_3$	–H	304	254.7–257.6	26.0	0.892–0.005	0.719–0.006
2	$-CH_3$	$-CH_3$	318	235.9 (dec.)	37.7	0.897–0.005	0.727–0.006
3	$-CH_3$	$-OCH_3$	334	260.2–262.3	48.8	0.853–0.006	0.675–0.007
4	$-CH_3$	$-NO_2$	349	226.3–227.5	90.1	0.835–0.006	0.653–0.007
5	$-CH_3$	$-NHCOCH_3$	361	276.3–278.6	52.2	0.819–0.006	0.633–0.007
6	$-CH_3$	–Cl	338	265.6–266.9	85.9	0.884–0.005	0.705–0.006
7	$-OCH_3$	–H	320	252.9–253.2	39.4	0.889–0.005	0.716–0.006
8	$-OCH_3$	$-CH_3$	334	215.2–216.9	33.3	0.863–0.006	0.684–0.007
9	$-OCH_3$	$-OCH_3$	350	230.7–232.9	69.3	0.894–0.005	0.724–0.006
10	$-OCH_3$	$-NO_2$	365	236.9–238.2	66.1	0.833–0.006	0.654–0.007
11	$-OCH_3$	$-NHCOCH_3$	377	245.3–249.9	75.6	0.809–0.006	0.628–0.007
12	$-OCH_3$	–Cl	354	162.1–163.8	51.0	0.882–0.005	0.703–0.006
13	$-OCH_2CH_3$	–H	334	270.0–271.0	41.2	0.880–0.005	0.709–0.006
14	$-OCH_2CH_3$	$-CH_3$	348	228.4–230.3	47.1	0.858–0.006	0.686–0.007
15	$-OCH_2CH_3$	$-OCH_3$	365	220.3–222.2	46.5	0.858–0.006	0.685–0.007
16	$-OCH_2CH_3$	$-NO_2$	379	247.9–248.9	71.2	0.817–0.006	0.651–0.007
17	$-OCH_2CH_3$	$-NHCOCH_3$	391	262.3–263.6	40.3	0.813–0.006	0.640–0.007
18	$-OCH_2CH_3$	–Cl	368	151.2–153.8	85.1	0.872–0.006	0.697–0.006
19	$-NO_2$	–H	335	241.5–248.9	37.6	0.888–0.005	0.679–0.007
20	$-NO_2$	$-CH_3$	349	178.1–179.6	18.8	0.860–0.006	0.640–0.007
21	$-NO_2$	$-OCH_3$	365	187.1–189.3	33.8	0.845–0.006	0.631–0.007
22	$-NO_2$	$-NO_2$	380	203.1–205.4	47.4	0.893–0.005	0.687–0.007
23	$-NO_2$	$-NHCOCH_3$	392	230.2–233.1	53.3	0.809–0.006	0.595–0.007
24	$-NO_2$	–Cl	369	218.9–2237	35.6	0.880–0.005	0.666–0.007
25	$-NO_2$	–F	353	163.3–164.1	34.4	0.861–0.006	0.638–0.007
26	–F	$-NO_2$	353	259.3–262.1	81.1	0.836–0.006	0.638–0.007
27	–Cl	$-NO_2$	369	244.9–249.5	58.2	0.881–0.005	0.697–0.006

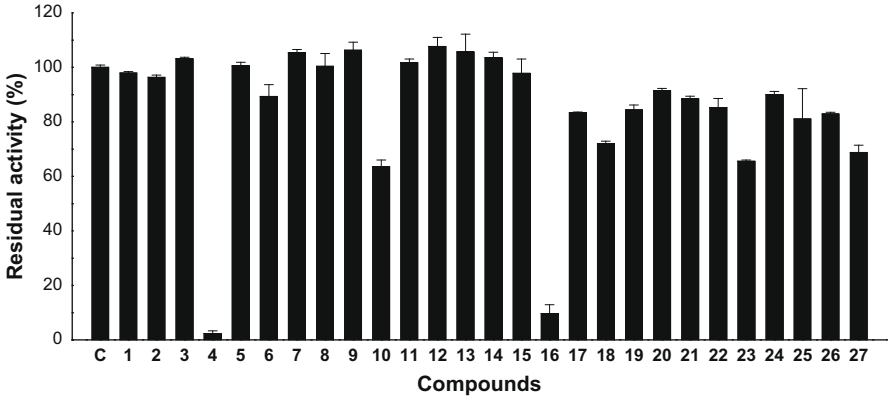

Figure 1. Inhibition of PTP-1B enzyme activity. Inhibition tests were assayed using a fixed substrate concentration, 2 mM pNPP, corresponding to the K_m value of the enzyme measured at pH 7.0. For each inhibitor the final concentration was 40 μM. Each test (final volume 1 ml) was started with 0.16 μg of PTP-1B. Control experiment (C) was carried out using DMSO. All tests were conducted in quadruplicate. The data represent the means ± S.E.M. Residual activity, expressed as%, is defined as the ratio between enzyme activity measured in the presence of the inhibitor and that of the control.

presence of a 125-fold molar excess of inhibitor for 1 h at two differing temperatures, 4 °C and 37 °C. Control experiments were conducted adding DMSO instead of inhibitor. After this interval time, the enzyme solutions were diluted 400-fold and the residual enzyme activity was assayed. The results are shown in Figure 2. In all cases the recovery of the activity was almost complete, suggesting that **4** and **16** behave as reversible inhibitors.

To assess the ability of compounds **4** and **16** to behave as slow-binding inhibitors, we studied the time-course of the PTP-1B-catalyzed hydrolysis of *p*-nitrophenyl phosphate in the presence of different inhibitor concentrations, monitoring continuously the release of *p*-nitrophenol at 400 nm. For both compounds we found that initial rates decrease with increasing inhibitor concentrations, and curves maintain linear monophasic behaviors as time progresses, indicating that the rapid equilibrium conditions occur in the formation of enzyme-inhibitor complexes. Identical behavior was found pre-incubating PTP-1B with inhibitors for 30 min before the activity assay (data not shown). Taken together our results suggest that both association and dissociation of inhibitors to the enzyme are rapid events, excluding the hypothesis that these compounds are slow-binding inhibitors.

Figures 3A and B show the concentration–response plots by compound **4** and compound **16**, respectively. The calculated IC_{50} values reported in Table 2 are in the low μM range. Thus our assay system is operated under non-tight binding conditions in the case of each inhibitor examined since IC_{50} is greater than fivefold over enzyme concentration (10 nM in all assays) and the approximation that [inhibitor] free = [inhibitor] total is valid.

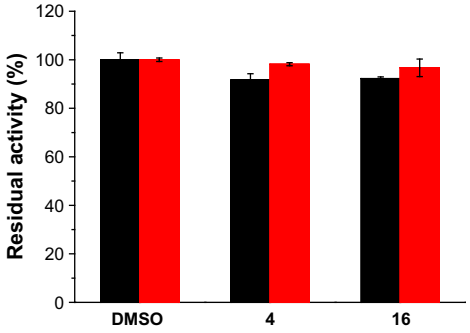

Figure 2. Inhibition reversibility assay. Aliquots of PTP-1B were incubated in the presence of 100 μM of each compound for 1 h at 4 °C (black bar) or 37 °C (red bar). Then, the enzyme was diluted 400-fold with the assay solution to measure the residual activity (37 °C, 5 mM pNPP). Control experiments were carried out adding DMSO. All tests were performed in triplicate. The data represent the mean ± S.E.M.

To verify if some compounds act as partial inhibitors, we measured the rate of PTP-1B-catalyzed hydrolysis of *p*-nitrophenyl phosphate at high substrate concentration (12.5-fold the K_m of the enzyme) in the presence of increasing concentrations of each compound. The results obtained for compounds **4** and **16** are reported in Figure 4. We observed that, by increasing the inhibitor concentration, the hydrolysis rate is reduced near to zero, suggesting that the binding of inhibitor to enzyme produces an inactive EI complex.

To determine the kinetic mechanism of inhibition, we analyzed experimental data by the double reciprocal plot method. For each compound, we measured the initial hydrolysis rate using a range of substrate final concentrations (0.5–40 mM), in the presence of increasing concentrations of each compound (Figs. 5–8).

The reciprocal plots for **4** and **16** showed straight lines that intersect each other in the left panel, suggesting that they are mixed-type inhibitors. This is confirmed by the fact that increasing inhibitor concentration is accompanied by the increase of K_m values and the decrease of V_{max} values (see Figs. 5–8). Wiesmann et al. reported a study on the inhibition of PTP-1B with a similar class of compounds. They also observed a similar inhibition type.[14]

For both mixed-type inhibitors we considered the model:

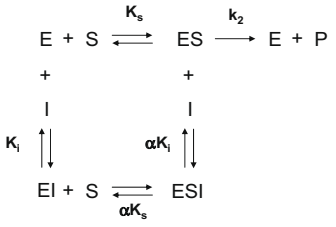

Thus we expected that the inhibitor binds to the free enzyme, E, and to the enzyme-substrate complex, ES. In this model EI has lower affinity for S than E ($\alpha > 1$), and ESI is non productive. We calculated the value of K_i (mixed-type) replotting the slope of the straight lines of the double reciprocal plot versus [I]. The results obtained in this experiment are reported in Table 3.

2.3. Docking studies with PTP-1B

In order to gain an insight into the binding mode of **4** and **16**, compounds were docked into the ligand binding pocket of human PTP-1B (PDB entry 2F71).[15] Docking was performed with the pro-

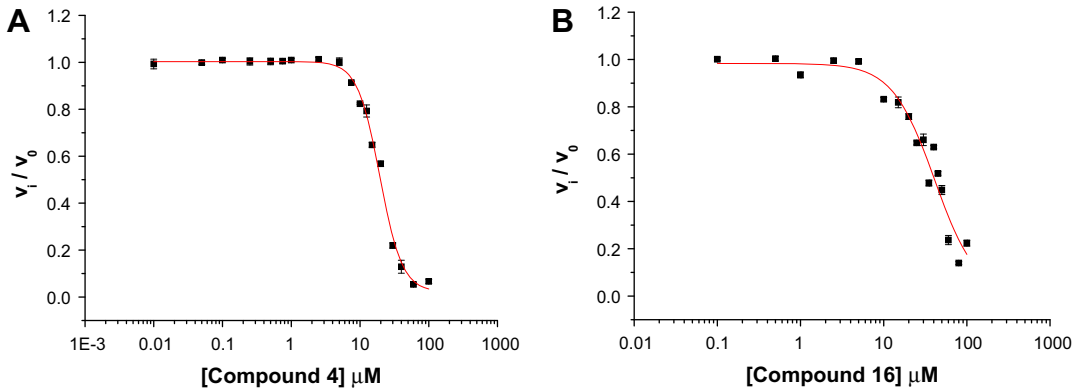

Figure 3. The IC_{50} values were determined by plotting the relative activity of PTP-1B versus inhibitor concentration (**4** graph A; **16** graph B). For each inhibitor, 15–18 different inhibitor concentrations were used. All tests were conducted in quadruplicate. The data represent the means ± S.E.M.

Table 2
IC_{50} values for compounds **4**, and **16**

Compound	IC_{50} (μM)
4	19.5 ± 1.0
16	40.9 ± 2.8

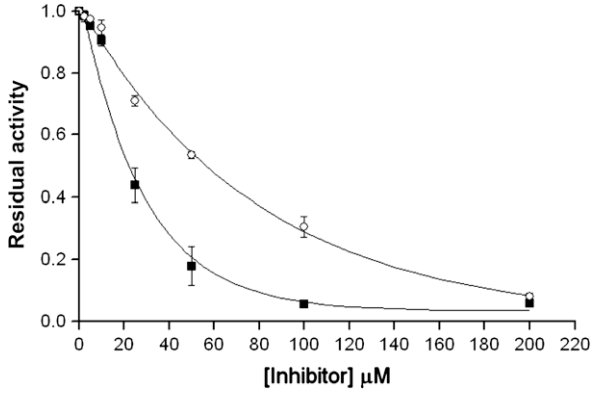

Figure 4. The residual enzyme activity was measured at 37 °C and pH 7.0 using 25 mM pNPP as substrate. The inhibitors concentrations used were: 2.5, 5.0, 10, 25, 50, 100 and 200 μM. The symbols are: **4**, ■; **16,** ○. All tests were performed in quadruplicate. The data represent the mean ± S.E.M.

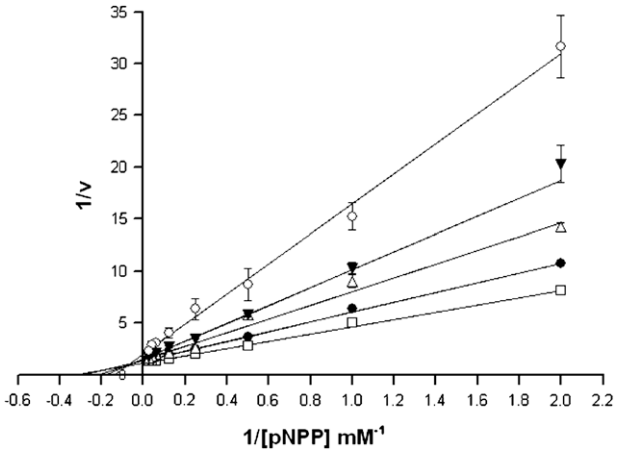

Figure 5. Compound **4**: double reciprocal plot ($1/v$ vs $1/[S]$). The concentrations of inhibitor were: 0 μM, □; 8 μM, ●; 12 μM, △; 16 μM, ▼; 20 μM, ○. All tests were conducted in quadruplicate. The data represent the means ± S.E.M.

gram AUTODOCK 3.0[16] using an automated flexible protocol as described in Section 4. Before docking **4** and **16**, the docking protocol was validated predicting the binding mode of the crystallographic 1,2,3,4-tetrahydroisoquinolinyl sulfamic acid.[15] AUTODOCK successfully predicted the binding mode of crystallographic ligand with RMS deviation of 1.09 Å.

After docking **4** and **16**, the binding pockets of the 2-arylsulfonylamino benzothiazoles were fully optimized. Figures 9A and B depict the top ranked binding modes after energy minimization. Figures 10A and B show the corresponding interaction diagram of the optimized models generated with the program Molecular Operating Environment (MOE).[17] According to the optimized complexes, the residues Tyr46, Arg47, Val49, Asp181, Phe182, Cys215, Ser216, Ala217, Arg221 and Gln262 are common to the binding pocket of **4** and **16**. Interestingly, Asp181, Cys215 and Arg221 are catalytic residues.[18] In both molecules, the nitro group at the arylsulfonylamino moiety is directed to the catalytic residues and it is immersed in a highly positive region.[19]

2.4. In vivo antihyperglycemic activity of 4 and 16

Compounds **4** and **16** were evaluated for in vivo antihyperglycemic activity using a STZ-nicotinamide rat model of T2DM.[21] Glibenclamide was taken as positive control.[7] The antihyperglycemic activity of both compounds was determined using a 100 mg/kg single dose. Compound **4** demonstrated important antihyperglycemic activity, by lowering glycemia ranging from 27% to 35%. The effect was consistent during the 7 h of experiment (Fig. 11). Compound **16** showed similar effects than glibenclamide, lowering the glycemia until 60% in this model of T2DM. The most pronounced effect of both compounds was observed during the first 5 h of post-intragastric administration of tested compounds, maintaining it until the 7th-h. These behavior could be related to pancreatic effects.

3. Conclusion

We have synthesized a small library of 2-arylsulfonylaminobenzothiazoles and evaluated these compounds for their protein tyrosine phosphatase-1B inhibitory activity. Several compounds of this series have shown significant PTP-1B inhibitory activity, in particular those that bear nitro group at position 4 of the sulfonamide moiety. Compounds **4** and **16** have exhibited most promising activity as mixed-type inhibitors of PTP-1B. The in vivo anti-hyperglycemic activities of these compounds make them a suitable leads to develop new chemical entities for potential use in the treatment of T2DM.

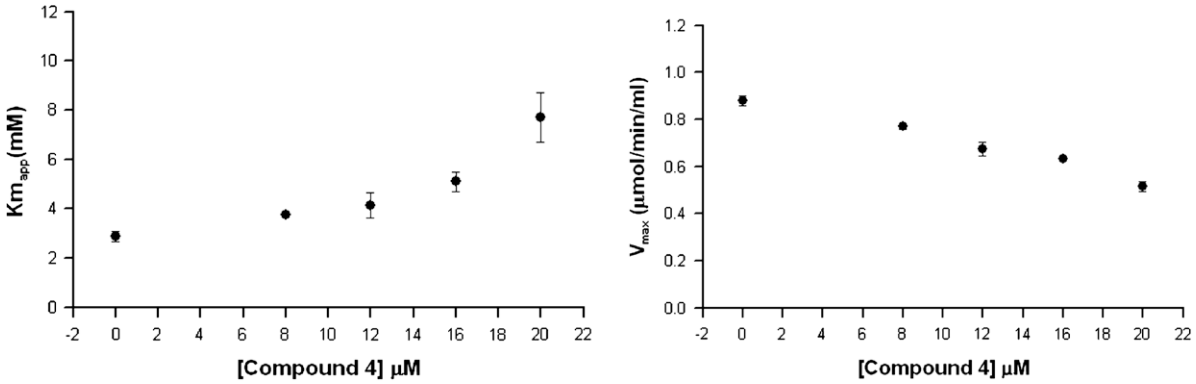

Figure 6. Dependence of main kinetic parameters K_m and V_{max} from the concentration of compound **4**. The concentrations of inhibitor used were: 0, 8, 12, 16 and 20 μM. The data represent the K_m or V_{max} values ± S.E.M.

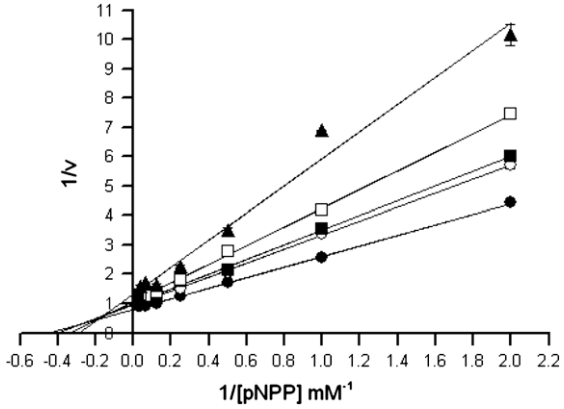

Figure 7. Compound **16**: double reciprocal plot ($1/v$ vs $1/[S]$). The concentrations of inhibitor used were: 0 μM, ●; 5 μM, ○; 10 μM, ■; 20 μM, □; 30 μM, ▲. All tests were conducted in quadruplicate. The data represent the means ± S.E.M.

Table 3
The inhibition constants for compounds **4** and **16**

Compound	K_i (μM)	α	Inhibition type
4	7.1 ± 1.0	4.8	Linear mixed-type
16	20.4 ± 3.7	2.5	Linear mixed-type

The data represent K_i values ± S.E.M.

4. Experimental

4.1. Chemistry

Melting points were determined on an EZ-Melt MPA120 automated melting point apparatus from Stanford Research Systems and are uncorrected. Reactions were monitored by TLC on 0.2 mm precoated Silica Gel 60 F254 plates (E. Merck). ^{1}H NMR spectra were recorded on a Varian INOVA 4008 (200 MHz) and ^{13}C NMR (50.28 MHz) instrument, and Varian Mercury 200 instruments. Chemical shifts are given in ppm relative to tetramethylsilane (Me_4Si, $\delta = 0$) in DMSO-d_6; J values are given in hertz. The following abbreviations are used: s, singlet; d, doublet; q, quartet; dd, doublet of doublet; t, triplet; m, multiplet; br s, broad signal. MS were recorded on a JEOL JMS-700 spectrometer by Fast Atom Bombarded [FAB (+)]. Predictive values of antidiabetic and antiobesity activities were also investigated using the chemistry software server PASS (http://195.178.207.233/PASS/).

Starting materials 6-substituted-1,3-benzothiazol-2-amines (**28–33**), and 4-substituted-benzenesulfonyl chlorides (**34–40**), were commercially available from Aldrich and used without purification.

4.1.1. General method of synthesis of derivatives 1–27

To a solution of 4-substituted benzenesulfonyl chloride (0.006 mol, 1.2 equiv) were added triethylamine (1.1 equiv), and a catalytic amount of 4-dimethylaminopyridine (DMAP) The reaction mixture was stirred at room temperature for 15 min. After, a solution of 2-amino-6-substituted benzothiazole (0.0030 mol) was added droopingly. The reaction mixture was stirred at 40 °C for 6–10 h. After complete conversion as indicated by TLC, the sol-

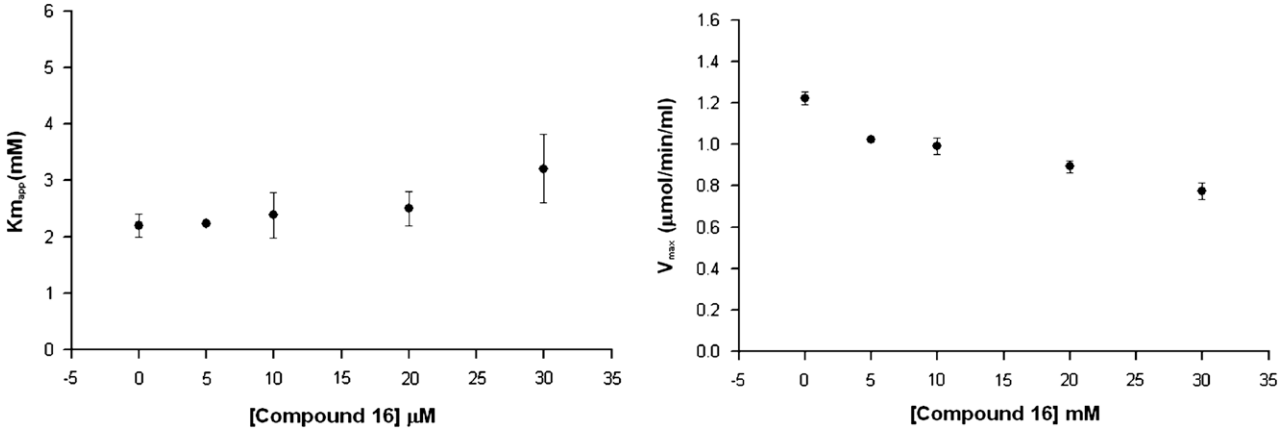

Figure 8. Dependence of main kinetic parameters K_m and V_{max} from the concentration of compound **16**. The concentrations of inhibitor used were: 0, 5, 10, 20, and 30 μM. The data represent the K_m or V_{max} values ± S.E.M.

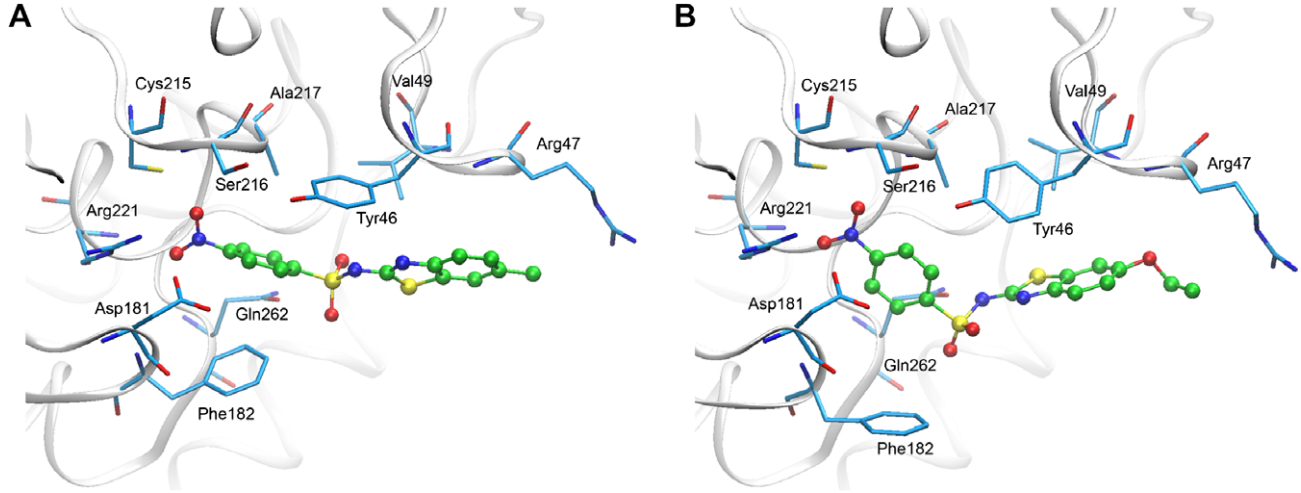

Figure 9. Predicted binding mode of **4** (A) and **16** (B), into the catalytic site of PTP-1B. Amino acid residues common to the binding pocket of both molecules (within 4.5 Å) are labeled. Figure generated with the program VMD 1.8.6.[20]

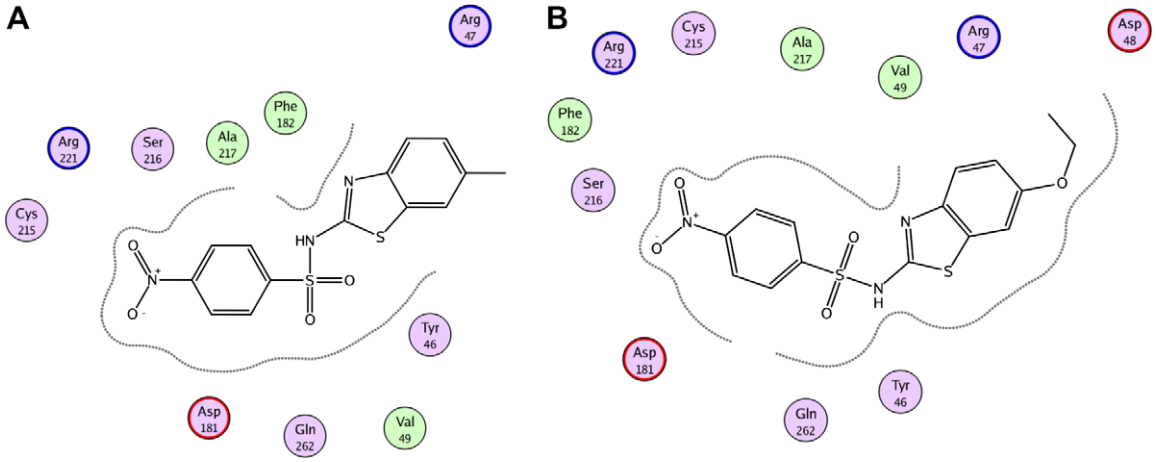

Figure 10. Two-dimensional interaction map of **4** (A) and **16** (B), docked into the PTP-1B catalytic pocket. Amino acid residues at 4.5 Å of the ligand are shown.

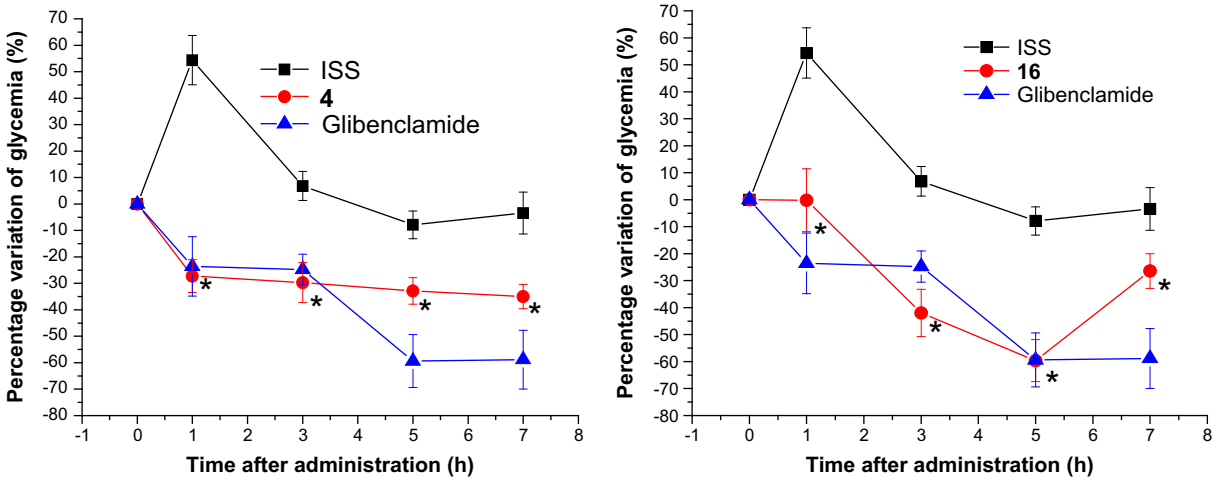

Figure 11. Effect of a single dose of **4** and **16** (100 mg/kg; intragastric, $n = 5$) in streptozotocin-nicotinamide rat model of diabetes. ISS: Isotonic saline solution. $^{*}p < 0.05$ versus ISS group.

vent was removed in vacuo, the residue was neutralized with saturated $NaHCO_3$ solution, and the aqueous layer was extracted with ethyl acetate (3 × 15 mL), washed with water (3 × 20 mL), and dried over anhydrous Na_2SO_4. The solvent was evaporated in vacuo and the precipitated solids were recrystallized from an appropriate solvent or purified by column chromatography.

4.1.1.1. *N*-(6-Methyl-1,3-benzothiazol-2-yl) benzenesulfonamide (1). White solid, yield 0.48 g (26.0%). Mp 254.7–257.6 °C. ^{1}H NMR (200 MHz, DMSO-d_6): δ 2.3 (s, 3H, CH_3), 7.2 (s, 2H, H-3′, H-5′), 7.5–7.6 (m, 3H, H7, H2′,H6′, J = 2.0, 5.8), 7.8–7.9 (br s, 2H, H-4, H-5′) ppm. ^{13}C NMR (50.28 MHz, DMSO-d_6):δ 20.8 (CH_3), 112.4 (C-7), 122.4 (C-4), 124.7 (C-7a), 125.7 (C-2′, C6′), 128.0 (C-5), 129.0 (C-3′, C-5′), 132.3 (C-4′), 133.1 (C-6), 133.9 (C-1′), 141.9 (C-3a), 166.7 (C-2) ppm; MS (FAB$^+$): m/z 305 (M+H)$^+$; Anal. Calcd for $C_{14}H_{12}N_2O_2S_2$: C, 55.24; H, 3.97; N, 9.20. Found: C, 55.18; H, 4.08; N, 8.87.

4.1.1.2. 4-Methyl-*N*-(6-methyl-1,3-benzothiazol-2-yl)benzenesulfonamide (2). White solid, yield 0.73 g (37.7%) Mp 235.9 (dec) °C. ^{1}H NMR (200 MHz, DMSO-d_6): δ 2.3 (s, 3H, CH_3), 2.3 (s, 3H, CH_3), 7.1–7.2 (m, 2H, H-3′, H-5′, J = 1.2, 8.0), 7.1 (d, 2H, H2′, H6′, J = 7.6), 7.5 (d, 2H, H-4, H-5 J = 8.0) ppm. ^{13}C NMR (50.28 MHz, DMSO-d_6): δ 20.4 (CH_3), 20.6 (CH_3),106.5 (C-7), 112.9 (C-4), 121.6 (C-7a), 125.4 (C-2′, C-6′), 125.5 (C-5), 128.9 (C-3′, C-5′), 131.9 (C-1′), 136.12 (C-6), 139.4 (C-4′), 141.6 (C-3a), 166.1 (C-2) ppm; MS(FAB$^+$): m/z 319 (M+H)$^+$; Anal. Calcd for $C_{15}H_{14}N_2O_2S_2$: C, 56.58; H, 4.43; N, 8.80. Found: C, 57.10; H, 4.69; N,9.86.

4.1.1.3. 4-Methoxy-*N*-(6-methyl-1,3-benzothiazol-2-yl)benzenesulfonamide (3). White solid, yield 1.08 g (48.8%) Mp 260.2–262.3 °C. ^{1}H NMR (200 MHz, DMSO-d_6): δ 2.3 (s, 3H, CH_3), 3.8 (s, 3H, –OCH_3), 7.1 (d, 2H, H-3′, H-5′, J = 8.0), 7.2 (m, 2H, H2′, H6′), 7.6 (br s, 1H, H-7), 7.8 (d, 2H, H4, H5, J = 8.8) ppm. ^{13}C NMR (50.28 MHz, DMSO-d_6): δ 20.4 (CH_3), 55.2 (OCH_3), 111.9 (C-7), 113.7 (C-3′, C-5′) 121.9 (C-4), 124.3 (C-7a), 127.5 (C-2′, C-6′), 127.6 (C-5), 132.6 (1′), 133.4 (C-6), 133.6 (C-3a), 161.6 (C-4′), 165.9 (C-2) ppm; MS(FAB$^+$): m/z 335 (M+H)$^+$; Anal. Calcd for $C_{15}H_{14}N_2O_3S_2$: C, 53.87; H, 4.24; N, 8.38. Found: C, 53.51; H, 4.35; N, 8.24.

4.1.1.4. N-(6-Methyl-1,3-benzothiazol-2-yl)-4-nitro benzenesulfonamide (4). Beige solid, yield 1.92 g (90.1%) of beige solid. Mp 226.3–227.5 °C. ^{1}H NMR (200 MHz, DMSO-d_6): δ 2.3 (s, 3H, CH_3), 7.2 (s, 2H, H-4, H-5), 7.6 (s, 1H, H-7), 8.1 (d, 2H, H-2′, H-6′, J = 8.8 Hz), 8.3 (d, 2H, H-3′, H-5′, J = 8.8 Hz) ppm. ^{13}C NMR (50.28 MHz, DMSO-d_6): δ 20.7 (CH_3), 112.8 (C-7), 122.4 (C-4), 124.4 (C-3′, C-5′), 124.9 (C-7a), 127.2 (C-2′, C-6′), 128.2 (C-5), 133.4 (C-6), 134.1 (C-1′), 147.3 (C-3a), 149.3 (C-4′), 167.3 (C-2) ppm; MS (FAB$^+$): m/z 350 (M+H)$^+$; Anal. Calcd for $C_{14}H_{11}N_3O_4S_2$: C, 48.13; H, 3.17; N, 12.03. Found: C, 47.38; H, 3.13; N, 12.16.

4.1.1.5. *N*-(4-{[(6-Methyl-1,3-benzothiazol-2-yl) amino]sulfonyl}phenyl)acetamide (5). White solid, yield 1.15 g (52.2%) Mp 276.3–278.6 °C. ^{1}H NMR (200 MHz, DMSO-d_6): δ 2.1 (s, 3H, $NHCOCH_3$), 3.4 (s, 3H, CH_3), 3.7 (s, 1H, NH), 7.3–7.4 (dd, 1H, H-5, J = 1.2, 8.8 Hz), 7.5–7.8 (m, 5H, H2′, H-3′, H-5′, H-6′, H-7), 8.2 (d, 1H, H-4, J = 8.8) ppm. ^{13}C NMR (50.28 MHz, DMSO-d_6): δ 20.5 ($NHCOCH_3$), 24.3 (CH_3), 115.5 (C-7), 118.1 (C-4), 118.2 (C-3′, C-5′) 122.7 (C-7a), 127.1 (C-2′, C-6′), 129.9 (C-5), 135.4 (C-1′), 143.4 (C-4′), 145.4 (C-3a), 168.8 (C-2), 169.1 ($NHCOCH_3$), ppm; MS (FAB$^+$): m/z 362 (M+H)$^+$; Anal. Calcd for $C_{16}H_{15}N_3O_3S_2$: C, 53.17; H, 4.18; N, 11.63. Found: C, 51.13; H, 4.30; N, 11.00.

4.1.1.6. 4-Chloro-*N*-(6-methyl-1,3-benzothiazol-2-yl)benzenesulfonamide (6). Yield 5.33 g (85.9%) of a white solid. Mp 265.6–266.9 °C. ^{1}H NMR (200 MHz, DMSO-d_6): δ 7.2 (s, 1H, H-7), 7.6 (m, 4H, H-2′, H-3′, H-5′, H-6′), 7.9 (m, 2H, H-4, H-5) ppm. ^{13}C NMR (50.28 MHz, DMSO-d_6): δ 20.8 (CH_3), 112.5 (C-7), 122.4 (C-4), 124.7 (C-7a), 127.7 (C-2′, C-6′), 128.1 (C-5), 129.1 (C-3′, C-5′), 133.3 (C-6), 133.9 (C-4′), 137.0 (C-3a), 140.8 (C-1′), 166.9 (C-2) ppm. MS (FAB$^+$): m/z 339 (M+H)$^+$; Anal. Calcd for $C_{14}H_{11}ClN_2O_2S_2$: C, 49.63; H, 3.27; N, 8.27. Found: C, 49.02; H, 3.13; N, 8.26.

4.1.1.7. *N*-(6-Methoxy-1,3-benzothiazol-2-yl) benzenesulfonamide (7). White solid, Yield 0.69 g (39.4%) of a white solid. Mp 252.9–253.2 °C ^{1}H NMR (200 MHz, DMSO-d_6): δ 6.9 (dd, 1H, H-5, J = 8.8, J = 2.2 Hz), 7.2 (d, 1H, H-4, J = 8.8 Hz), 7.4 (d, 1H, H-7, J = 2.2 Hz), 7.4–7.6 (m, 3H, H-′, H-4′, H-5′), 7.8 (m, 2H, H-2′, H-6′) ppm. ^{13}C NMR (50.28 MHz, DMSO-d_6): δ 55.7 (CH_3O), 106.9 (C-7), 113.4 (C-5), 114.6 (C-4), 125.6 (C-2′, C-6′), 125.9 (C-7a), 129.1 (C-3′, C-5′), 129.7 (C-4′), 132.2 (C-1′), 142.0 (C-4a), 155.9 (C-6), 166.4 (C-2). MS (FAB$^+$): m/z 321 (M+H)$^+$; Anal. Calcd for $C_{14}H_{12}N_2O_3S_2$: C, 52.48; H, 3.78; N, 8.74. Found: C, 52.29; H, 3.65; N, 8.98.

4.1.1.8. N-(6-Methoxy-1,3-benzothiazol-2-yl)-4-methylbenzenesulfonamide (8). Beige solid, yield 0.61 g (33.3%) Mp 215.2–216.9 °C. ^{1}H NMR (200 MHz, DMSO-d_6): δ 2.3 (s, 3H, CH_3), 3.8 (s, 3H, OCH_3), 6.9 (dd, 1H, H5, J = 2.6, 8.8 Hz), 7.2 (d, 1H, H4, J = 8.8 Hz), 7.3 (d, 2H, H3′, H5′, J = 8.0 Hz), 7.4 (d, 1H, H7, J = 2.6 Hz), 7.7 (d, 2H, H2′, H6′, J = 8.4 Hz) ppm. ^{13}C NMR (50.28 MHz, DMSO-d_6): δ 20.9 (CH_3), 55.7 (OCH_3), 106.9 (C-7), 113.4 (C-5), 114.6 (C-4), 125.7 (C-2′, C-6′), 125.9 (C-7a), 129.4 (C-3′, C-5′), 129.8 (C-1′), 139.2 (C-3a), 142.4 (C-4′), 155.9 (C-6), 166.2 (C-2) ppm; MS(FAB$^+$): m/z 335 (M+H)$^+$; Anal. Calcd for $C_{15}H_{14}N_2O_3S_2$: C, 53.87; H, 4.22; N, 8.38. Found: C, 53.63; H, 4.11; N, 8.00.

4.1.1.9. 4-Methoxy-*N*-(6-methoxy-1,3-benzothiazol -2-yl)benzenesulfonamide (9). Beige solid, yield 1.34 g (69.3%) Mp 230.7–232.9 °C. ^{1}H NMR (200 MHz, DMSO-d_6): δ 3.8 (s, 3H, OCH_3), 3.8 (s, 3H, OCH_3), 6.9 (dd, 1H, H5, J = 2.2, 8.8 Hz), 7.0–7.1 (m, 2H, H3′, H5′, J = 1.8, 7.0 Hz), 7.2 (d, 1H, H4, J = 8.8 Hz), 7.4 (d, 1H, H7, J = 2.2 Hz), 7.7–7.8 (m, 2H, H2′, H6′, J = 2.2, 7.0 Hz) ppm. ^{13}C NMR (50.28 MHz, DMSO-d6): δ 65.2 (OCH_3), 65.3 (OCH_3), 116.6 (C-7), 122.9 (C-5), 123.8 (C-3′, C-5′), 124.2 (C-4), 135.5 (C-7a), 137.4 (C-2′, C-6′), 139.4 (C-1′), 143.5 (C-3a), 165.5 (C-6), 171.6 (C-4′), 175.6 (C-2) ppm; MS(FAB$^+$): m/z 351 (M+H)$^+$; Anal. Calcd for $C_{15}H_{14}N_2O_4S_2$: C, 51.14; H, 4.03; N, 7.99. Found: C, 50.99; H, 4.190; N, 7.91.

4.1.1.10. *N*-(6-Methoxy-1,3-benzothiazol-2-yl)-4-nitrobenzenesulfonamide (10). Yield 1.33 g (66.1%) of a yellow solid. Mp 236.9–238.2 °C. ^{1}H NMR (200 MHz, DMSO-d_6): δ 3.8 (s, 3H, CH_3O), 7.0 (dd, 1H, H-5 J = 8.8, J = 2.2 Hz), 7.2 (d, 1H, H-4, J = 8.8 Hz), 7.5 (d, 1H, H-7, J = 2.2 Hz), 8.1 (d, 2H, H-2′, H-6′, J = 8.4 Hz), 8.4 (d, 2H, H-3′, H-5′, J = 8.8 Hz) ppm; ^{13}C NMR (50.28 MHz, DMSO-d_6) δ 55.7 (CH_3), 106.9 (C-7), 113.8 (C-5), 114.9 (C-4), 124.4 (C-3′, C-5′), 126.0 (C-7a), 127.2 (C-2′, C-6′), 129.7 (C-3a), 147.3 (C-1′), 149.3 (C-4′), 156.2 (C-6), 167.0 (C-2) ppm; MS (FAB$^+$): m/z 366 (M+H)$^+$; Anal. Calcd for $C_{14}H_{11}N_3O_5S_2$: C, 46.02; H, 3.03; N, 11.50;. Found: C, 45.75; H, 2.93; N, 11.77.

4.1.1.11. *N*-(4-{[(6-Methoxy-1,3-benzothiazol-2-yl)amino]sulfonyl}phenyl)acetamide (11). Beige solid, yield 1.57 g (75.6%) Mp 245.3–249.9 °C. ^{1}H NMR (200 MHz, DMSO-d_6): δ 2.1 (s, 3H, NHC-OCH_3), 3.8 (s, 3H, OCH_3), 5.8 (s, 1H, NH), 7.0 (dd, 1H, H5, J = 2.6, 8.8 Hz), 7.2 (d, 1H, H4, J = 8.8 Hz), 7.4 (d, 1H, H7, J = 2.4 Hz), 7.5–7.8 (m, 4H, H2′, H3′, H5′, H6′, J = 1.8, 2.6, 9.2 Hz), 10.3 (s, 1H, NHC-OCH_3) ppm. ^{13}C NMR (50.28 MHz, DMSO-d_6): δ 24.1 ($NHCOCH_3$), 55.7 (OCH_3), 107.0 (C-7), 113.4 (C-5), 114.6 (C-4), 118.4 (C-3′, C-5′), 126.0 (C-7a), 126.9 (C-2′, C-6′), 129.8 (C-1′) 135.7 (C-4′),

142.6 (C-3a), 155.9 (C-6), 166.1 ($NHCOCH_3$), 168.8 (C-2) ppm; MS(FAB^+): m/z 378 $(M+H)^+$; Anal. Calcd for $C_{16}H_{15}N_3O_4S_2$: C, 50.91; H, 4.01; N, 11.13. Found: C, 49.42; H, 4.21; N, 10.19.

4.1.1.12. 4-Chloro-*N*-(6-methoxy-1,3-benzothiazol-2-yl)benzenesulfonamide (12). Beige solid, yield 0.99 g (51.0%) Mp 162.1–163.8 °C. ^1H NMR (200 MHz, DMSO-d_6): δ 3.8 (s, 3H, OCH_3), 7.0 (dd, 1H, H-5, J = 2.6, 8.8 Hz), 2.3 (d, 1H, H-4, J = 8.8 Hz), 7.3 (d, 1H, H-7, J = 2.6 Hz), 7.6–7.7 (m, 2H, H-2′, H-6′), 7.8–7.9 (m, 2H, H-3′, H-5′) ppm. ^{13}C NMR (50.28 MHz, DMSO-d_6): δ 55.7 (OCH_3), 106.9 (C-7), 113.7 (C-5), 114,7 (C-4), 127.6 (C-2′, C-6′), 129.1 (C-3′, C-5′), 129.9 (C-7a), 137.0 (C-4′), 140.9 (C-3a), 156.0 (C-6), 166.5 (C-2) ppm; MS(FAB^+): m/z 355 $(M+H)^+$; Anal. Calcd for $C_{14}H_{11}N_2O_3S_2Cl$: C,47.39; H, 3.12; N, 8.89. Found: C, 47.68; H, 3.31; N, 8.90.

4.1.1.13. *N*-(6-Ethoxy-1,3-benzothiazol-2-yl)benzenesulfonamide (13). White solid, yield 0.39 g (41.2%) Mp 270.0–271.0 °C. ^1H NMR (200 MHz, DMSO-d_6): δ 1.2 (s, 3H, CH_3), 3.9 (q, 2H, OCH_2CH_3), 5.7 (s, 1H, NH), 6.9 (dd, 1H, H-5, J = 2.6, 8.8 Hz), 7.1 (d, 1H, H-4, J = 8.8), 7.3 (d, 1H, H-7, J = 2.2 Hz), 7.4–7.5 (m, 3H, H-3′, H-4′, H-5′), 7.7–7.8 (m, 2H, H-2′, H-6′, J = 1.4, 8.0 Hz) ppm. ^{13}C NMR (50.28 MHz, DMSO-d_6): δ 14.6 (OCH_2CH_3), 63.7 (OCH_2CH_3), 107.6 (C-7), 113.5 (C-5), 115.1 (C-4), 125.7 (C-2′, C-6′), 125.9 (C-7a), 129.0 (C-3′, C-5′), 129.7 (C-4′), 132.2 (C-1′), 142.0 (C-3a), 155.2 (C-6), 166.4 (C-2) ppm; MS(FAB^+): m/z 335 $(M+H)^+$; Anal. Calcd for $C_{15}H_{14}N_2O_3S_2$: C, 53.87; H, 4.22; N, 8.38. Found: C, 53.67; H, 4.15; N, 8.56.

4.1.1.14. *N*-(6-Ethoxy-1,3-benzothiazol-2-yl)-4-methylbenzenesulfonamide (14). Yield 0.92 g (47.1%) of beige solid. Mp 228.4–230.3 °C. ^1H NMR (200 MHz, DMSO-d_6): δ 1.3 (t, 3H, CH_3), 2.3 (s, 3H, CH_3O), 4.0 (q, 2H, CH_2O), 6.9 (dd, 1H, H-5, J = 8.8. J = 2.6 Hz), 7.2 (d, 1H, H-4, J = 8.8 Hz), 7.3 (d, 2H, H-3′, H-5′, J = 8.0 Hz), 7.4 (d, 1H, H-7, J = 2.6 Hz), 7.7 (d, 2H, H-3′, H-7′, J = 8.2 Hz) ppm; ^{13}C NMR (50.28 MHz, DMSO-d_6) δ 14.3 (CH_3), 20.6 (CH_3), 63.3 (CH_2), 107.1 (C-7), 113.1 (C-4), 114.6 (C-7a), 125.3 (C-2′, C-6′), 125.5 (C-5), 129.0 (C-3′, C-5′), 130.0 (C-6), 138.8 (C-1′), 142.0 (C-4′), 154.7 (C-3a), 165.8 (C-2) ppm. MS (FAB^+): m/z 349 $(M+H)^+$; Anal. Calcd. for $C_{16}H_{16}N_2O_3S_2$: C, 55.15; H, 4.63; N, 8.04. Found: C, 54.20; H, 4.40; N, 8.04.

4.1.1.15. *N*-(6-Ethoxy-1,3-benzothiazol-2-yl)-4-methoxybenzenesulfonamide (15). Beige solid, yield 1.5 g (46.5%) Mp 220.3–222.2 °C. ^1H NMR (200 MHz, DMSO-d_6): δ 1.3 (t, 3H, OCH_2CH_3), 3.8 (s, 3H, OCH_3), 4.0 (q, 2H, OCH_2CH_3), 6.9 (dd, 1H, H5, J = 2.2, 8.8 Hz), 7.1 (d, 2H, H3′, H5′, J = 8.8 Hz), 7.2 (d, 1H, H4, J = 8.8 Hz), 7.4 (d, 1H, H7, J = 2.4 Hz), 7.8 (d, 2H, H2′, H6′, J = 8.4 Hz) ppm. ^{13}C NMR (50.28 MHz, DMSO-d_6): δ 14.6 (OCH_2CH_3), 55.6 (OCH_3), 63.7 (OCH_2CH_3), 107.5 (C-7), 113.4 (C-5), 114.1 (C-3′, C-5′), 115.0 (C-4), 125.9 (C-7a), 127.8 (C-2′, C-6′), 133.9 (C-1′), 155.1 (C-3a), 161.9 (C-6), 166.0 (C-4′), 186.2 (C-2) ppm; MS(FAB^+): m/z 366 (M+H)+; Anal. Calcd for $C_{16}H_{16}N_2O_4S_2$: C, 52.73; H, 4.43; N, 7.69. Found: C, 52.41; H, 4.56, N,7.50.

4.1.1.16. *N*-(6-Ethoxy-1,3-benzothiazol-2-yl)-4-nitrobenzene sulfonamide (16). Yield 1.51 g (71.2%) of a yellow solid. Mp 247.9–248.9 °C. ^1H NMR (200 MHz, DMSO-d_6): δ 1.3 (t, 3H, CH_3), 4.0 (q, 2H, CH_2O), 7.0 (dd, 1H, H-5, J = 8.8, J = 2.6 Hz), 7.2 (d, 1H, H-4, J = 8.8 Hz), 7.5 (d, 1H, H-7, J = 2.2 Hz), 8.0–8.1 (m, 2H, H-2′, H-6′), 8.3- 8.4 (m, 2H, H-3′, H-5′) ppm; ^{13}C NMR (50.28 MHz, DMSO-d_6) δ 14.3 (CH_3), 63.4 (CH_2O), 107.2 (C-4), 113.5 (C-7), 124.1 (C-3′, C-5′), 126.9 (C-2′, C-6′), 129.3 (C-5), 147.0 (C-7a), 148.9 (C-6), 155.1 (C-1′), 166.7 (C-4′), 171.9 (C-3a), 172.8 (C-2) ppm; MS (FAB^+): m/z 380 $(M+H)^+$; Anal. Calcd For $C_{15}H_{13}N_3O_5S_2$: C, 47.48; H, 3.45; N, 11.08. Found: C, 46.88; H, 3.33; N, 11.26.

4.1.1.17. *N*-(4-{[(6-Ethoxy-1,3-benzothiazol-2-yl)amino]sulfonyl}phenyl)acetamida (17). White solid, yield 0.88 g (40.3%) Mp 262.3–263.6 °C. ^1H NMR (200 MHz, DMSO-d_6): δ 1.3 (t, 3H, OCH_2CH_3), 2.1 (t, 3H,$NHCOCH_3$), 4.0 (q, 2H, OCH_2CH_3), 5.8 (s, 1H, NH), 6.9 (dd, 1H, H-5, J = 2.4, 8.8 Hz), 7.2 (d, 1H, H-4, J = 8.8), 7.4 (d, 1H, H-7, J = 2.2 Hz), 7.6–7.8 (m, 4H, H-2′, H-3′, H-5′, H-6′, J = 3.2, 8.8 Hz), 10.3 (s, 1H, NH) ppm. ^{13}C NMR (50.28 MHz, DMSO-d_6): δ 24.1 (OCH_2CH_3), 30.7 ($NHCOCH_3$), 63.7 (OCH_2CH_3), 107.5 (C-7), 113.5 (C-5), 115.0 (C-4), 118.4 (C-3′, C-5′), 126.9 (C-3′, C-5′), 130.0 (C-7a), 135.8 (C-1′), 142.6 (C-3a),142.8 (C-4′), 155.1 (C-6), 166.1 (C-2), 168.8 ($NHCOCH_3$) ppm; MS(FAB^+): m/z 392 $(M+H)^+$; Anal. Calcd for $C_{17}H_{17}N_3O_4S_2$: C, 52.16; H, 4.38; N, 10.73. Found: C, 51.29; H, 4.51; N, 10.22.

4.1.1.18. 4-Chloro-*N*-(6-ethoxy-1,3-benzothiazol-2-yl)benzenesulfonamide (18). White solid, yield 1.75 g (85.01%) Mp 151.2–153.8 °C. ^1H NMR (200 MHz, DMSO-d_6): δ 3.0 (s, 3H, OCH_2CH_3), 4.0 (q, 2H, OCH_2CH_3), 7.0 (dd, 1H, H-5, J = 2.6, 7.8 Hz) 7.3 (d, 1H, H-4, J = 8.8 Hz), 7.4 (s, 1H, H-5), 7.6 (d, 2H, H-2′, H-6′, J = 8.8 Hz), 7.8 (d, 2H, H-3′, H-5′, J = 7.8 Hz) ppm. ^{13}C NMR (50.28 MHz, DMSO-d_6) δ: 14.6 (OCH_2CH_3), 63.7 (OCH_2CH_3), 107.5 (C-7), 113.7 (C-5), 115.1 (C-4), 125.9 (C-7a), 127.6 (C-2′, C-6′),129.1 (C-3′y C-5′), 136.9 (C-4′), 140.9 (C-3a), 155.24 (C-6), 166.4 (C-2) ppm; MS(FAB^+): m/z 369 (M+H)+; Anal. Calcd for $C_{15}H_{13}N_2O_3S_2Cl$: C, 48.84; H, 3.55; N, 7.59. Found: C, 48.32; H, 3.56; N, 7.45.

4.1.1.19. benzenesulfonamide (19)(19). Yellow solid, yield 0.64 g (37.6%) Mp 241.5–248.9 °C. ^1H NMR (200 MHz, DMSO-d_6): δ 7.4 (d, 1H, H4, J = 9.2 Hz), 7.5–7.6 (m, 3H, H3′, H4′, H5′), 7.8–7.9 (m, 2H, H2′, H6′), 8.2 (dd, 1H, H5, J = 2.6, 8.8 Hz), 8.8 (d, 1H, H7, J = 1.8 Hz) ppm. ^{13}C NMR (50.28 MHz, DMSO-d_6): δ 112.8 (C-7), 119.3 (C-5), 123.2 (C-4), 125.8 (C-2′, C-6′), 126.7 (C-7a), 129.2 (C-3′, C-5′), 132.7 (C-4′) 141.3 (C-1′), 141.6 (C-3a), 142.9 (C-6), 168.3 (C-2) ppm; MS(FAB^+): m/z 336 (M+H)+; Anal. Calcd for $C_{13}H_9N_3O_4S_2$: C, 46.56; H, 2.70; N, 12.53. Found: C, 46.26; H, 2.90; N, 11.89.

4.1.1.20. 4-Methyl-*N*-(6-nitro-1,3-benzothiazol-2-yl)benzenesulfonamide (20). Yellow solid, yield 0.34 g (18.8%) Mp 178.1–179.6 °C. ^1H NMR (200 MHz, DMSO-d_6): δ 2.1 (s, 3H, CH_3), 5.8 (s, 1H, N-H), 7.3 (d, 1H, H-4, J = 8.4 Hz), 7. 5 (dd, 1H, H-5, J = 2.2, 8.4 Hz), 7.9 (d, 1H, H-7, J = 1.8 Hz), 8.1 (d, 2H, H-3′, H-5′, J = 8.8 Hz), 8.4 (d, 2H, H2′, H6′, J = 8.8 Hz) ppm. ^{13}C NMR (50.28 MHz, DMSO-d_6): δ 20.7 (CH_3), 114.4 (C-7), 122.4 (C-4), 124.5 (C-2′, C-6′), 126.8 (C-5), 127.3 (C-3′, C-5′), 127.4 (C-7a), 127.9 (C-1′), 135.3 (C-6), 147.1 (C-4′), 149.4 (C-3a), 167.8 (C-2) ppm; MS(FAB^+): m/z 350 (M+H)+; Anal. Calcd for $C_{14}H_{11}N_3O_4S_2$: C, 48.13; H, 3.17; N, 12.03. Found: C, 49.00; H, 3.17; N, 12.00

4.1.1.21. 4-Methoxy-*N*-(6-nitro-1,3-benzothiazol-2-yl)benzene sulfonamide (21). Yield 0.63 g (33.8%) of yellow solid. Mp 187.1–189.3 °C. ^1H NMR (200 MHz, DMSO-d_6): δ 3.8 (s, 3H, CH_3O), 7.1 (d, 2H, H-3′, H-5′, J = 8.0), 7.8 (d, 2H, H2′, H6′, J = 8.4), 8.2 (sa, 2H, H-4, H-5), 8.8 (s, 1H, H-7) ppm. ^{13}C NMR (50.28 MHz, DMSO-d_6): δ 55.7 (CH_3), 114.3 (C-3′, C-5′), 119.1 (C-7), 123.1 (C-5), 126.3 (C-4), 126.9 (C-7a), 127.9 (C-2′, C-6′), 133.1 (C-1′), 138.9 (C-6), 142.8 (C-3a), 162.3 (C-4′), 167.8 (C-2) ppm; MS (FAB^+): m/z 366 $(M+H)^+$; Anal. Calcd for $C_{14}H_{11}N_3O_5S_2$: C, 46.02; H, 3.03; N, 11.50. Found: C, 46.49; H, 3.83; N, 10.94.

4.1.1.22. 4-Nitro-*N*-(6-nitro-1,3-benzothiazol-2-yl)benzenesulfonamide (22). Yellow solid, yield 0.92 g (47.4%) Mp 203.1–205.4 °C. ^1H NMR (200 MHz, DMSO-d_6): δ 7.5 (d, 1H, H-5, J = 8.8 Hz), 8.1 (d, 2H, H-2′, H-6′, J = 8.4 Hz), 8.3 (d, 1H, H-4, J = 8.8 Hz), 8.4 (d, 2H, H-3′, H-5′, J = 8.4 Hz), 8.9 (s, 1H, H-7) ppm.

^{13}C NMR (50.28 MHz, DMSO-d_6): δ 113.3 (C-7), 119.4 (C-4), 123.3 (C-5), 124.6 (C-3′, C-5′), 126.3 (C-7a), 127.4 (C-2′, C-6′), 141.8 (C-6), 143.2 (C-1′), 146.7 (C-4′), 149.6 (C-3a), 169.3 (C-2) ppm; MS(FAB$^+$): m/z 381 (M+H)$^+$; Anal. Calcd for $C_{13}H_8N_4O_6S_2$: C, 41.05; H, 2.12; N, 14.73. Found: C, 40.83; H, 2.40; N, 13.90.

4.1.1.23. *N*-(4-{[(6-Nitro-1,3-benzothiazol-2-yl)amino]sulfonyl}-phenyl)acetamide (23). Yield 1.07 g (53.3%) of a yellow solid. Mp 230.2–233.1 °C. ^{1}H NMR (200 MHz, DMSO-d_6): δ 2.9 (s, 3H, CH_3CO), 7.8 (d, 2H, H-4, H-5, J = 8.8), 8.5 (s, 1H, NH), 8.7 (s, 4H, H-2′, H-3′, H-5′, H-6′), 9.1 (s, 1H, H-7) ppm. ^{13}C NMR (50.28 MHz, DMSO-d_6): δ 23.9 (CH_3), 116.9 (C-7),116.9 (C-5), 117.7 (C-3′,C-5′), 118.0 (C-4), 121.9 (C-7a), 122.0 (C-2′, C-6′), 131.6 (C-1′), 140.7 (C-4′), 153.6 (C-6), 158.5 (C-3a), 163.3 (CO), 171.8 (C-2) ppm; MS(FAB$^+$): m/z 393 (M+H)$^+$; Anal. Calcd for $C_{15}H_{12}N_4O_5S_2$: C, 45.91; H, 3.08; N, 14.28. Found: C, 45.91; H, 3.08; N, 14.28.

4.1.1.24. 4-Chloro-*N*-(6-nitro-1,3-benzothiazol-2-yl)benzene-sulfonamide (24). Yellow solid, yield 0.67 g (35.6%). Mp 218.9–2237 °C. ^{1}H NMR (200 MHz, DMSO-d_6): δ 7.6–7.7 (M, 2H, H-3′, H-5′, J= 2.2, 8.8 Hz), 7.8–7.9 (m, 2H, H-2′, H-6′, J = 2.2, 8.8 Hz), 8.3 (dd, 2H, H-4, H-5, J = 2.2, 8.8 Hz), 8.9 (d, 1H, H-7, J = 2.6 Hz) ppm. ^{13}C NMR (50.28 MHz, DMSO-d_6): δ 112.9 (C-7), 119.3 (C-5), 123.2 (C-4), 126.2 (C-7a), 127.8 (C-2′, C-6′), 129.3 (C-3′, C-5′), 137.5 (C-4′), 140.2 (C-1′), 141.6 (C-6), 143.1 (C-3a), 168.6 (C-2) ppm; MS(FAB$^+$): m/z 370 (M+H)$^+$; Anal. Calcd for $C_{13}H_8N_3O_4S_2Cl$: C, 44.22; H, 2.18; N, 11.36. Found: C, 42.08; H, 2.30; N, 11.22.

4.1.1.25. 4-Fluoro-*N*-(6-nitro-1,3-benzothiazol-2-yl)benzene-sulfonamide (25). Yellow solid, yield 0.62 g (34.4%) Mp 163.3–164.1 °C. ^{1}H NMR (200 MHz, DMSO-d_6): δ 7.3 (d, 1H, H-4, J = 8.4 Hz), 7.5 (dd, 1H, H-5, J = 2.2, 8.4 Hz), 7.9 (d, 1H, H-7, J = 1.8 Hz), 8.1 (d, 2H, H-3′, H-5′, J = 8.8 Hz), 8.4 (d, 2H, H-2′, H-6′, J = 8.8 Hz) ppm. ^{13}C NMR (50.28 MHz, DMSO-d_6): δ 116.1–116.5 (C-3′, C-5′, J = 22.7 Hz), 117.8 (C-7), 120.2 (C-5), 122.7 (C-4), 125.4 (C-7a), 128.7- 128.9 (C-2′,C-6′, J = 9.5 Hz), 135.3 (C-1′), 137.7–143.0 (C-4′, J = 262.5 Hz), 145.7 (C-6), 155.1 (C-3a), 174.5 (C-2) ppm; MS(FAB$^+$): m/z 354 (M+H)+; Anal. Calcd for $C_{13}H_8N_3O_4S_2F$: C, 44.19; H, 2.28; N, 11.89. Found: C, 44.41; H, 2.19; N, 11.62.

4.1.1.26. *N*-(6-Fluoro-1,3-benzothiazol-2-yl)-4-nitrobenzene-sulfonamide (26). Yellow solid, 0.83 g (81.1%) Mp 259.3–262.1 °C. ^{1}H NMR (200 MHz, DMSO-d_6): δ 7.19–7.35 (m, 2H, H-4, H-7), 7.78 (dd, 1H, H-5′, J = 1.0, 8.0 Hz), 8.05–8.09 (m, 2H, H-3′, H-5′, J = 1.2 y 8.8 Hz), 8.33–8.37 (m, 2H, H-2′, H-6′, J = 1.2, 8.8 ppm. ^{13}C NMR (50.28 MHz, DMSO-d_6): δ 108.1 (C-7), 113.9 (C-5), 121.4 (C-3′, C5′), 123.4 (C-4), 126.1 (C-7a), 128.2 (C-2′, C-6′), 144.6 (C-3a), 145.8 (C-1′), 151.6 (C-4′), 158.6 (C-6), 174.5 (C-2) ppm; MS(FAB$^+$): m/z 354 (M+H)$^+$; Anal. Calcd for $C_{13}H_8N_3O_4S_2F$: C, 44.19; H, 2.28; N, 11.89. Found: C, 43.77; H, 2.30; N,11.48.

4.1.1.27. N-(6-Chloro-1,3-benzothiazol-2-yl)-4-nitrobenzene-sulfonamide (27). Yellow solid, yield 1.16 g (58.2%) Mp 244.9–249.5 °C. ^{1}H NMR (200 MHz, DMSO-d_6): δ 7.30 (d, 1H, H4, J = 8.8 Hz), 7.44 (dd, 1H, H5, J = 1.8, 8.4 Hz), 7.99 (d, 1H, J = 1.8 Hz), 8.07–8.12 (m, 2H, H2′, H6′, J = 1.8, 8.8 Hz), 8.35- 8.39 (m, 2H, H3′, H5′, J = 8.8 Hz) ppm. ^{13}C NMR (50.28 MHz, DMSO-d_6): δ 114.34 (C-7), 112.41 (C-4), 124.51 (C-3′, C-5′), 126.73 (C-5), 127.29 (C-2′, C-6′), 127.39 (C-7a), 127.86 (C-6), 135.23 (C-1′), 147.03 (C-3a), 149.41 (C-4′), 167.75 (C-2) ppm; MS(FAB$^+$): m/z 370 (M+H)+; Anal. Calcd for $C_{13}H_{11}N_2O_2S_2Cl$: C, 44.22; H, 2.18; N, 11.36. Found: C, 44.20; H, 2.18; N, 11.35.

4.2. Biological assays

4.2.1. PTP-1B expression and purification

All experiments were conducted using human recombinant PTP-1B. Briefly, the complete sequence of PTP-1B was cloned in the pGEX-2T bacterial expression vector downstream the GST sequence. This vector was used to transform *Escherichia coli* TB1 strain cells. The recombinant fusion protein was purified from bacterial lysate using a single-step affinity chromatography. The solution containing purified fusion protein was treated with thrombin for 3 h at 37 °C. Then the PTP-1B was purified from GST and thrombin by gel filtration on a Superdex G75 column. The purity of PTP-1B preparation was assessed by SDS–polyacrylamide gel electrophoresis.

4.2.2. Enzyme assays[13]

All assays were carried out at 37 °C. The substrate (*p*-nitrophenylphosphate) was dissolved in 0.075 M of β,β-dimethylglutarate buffer pH 7.0, containing 1 mM EDTA and 1 mM dithiothreitol. The final volume was 1 ml. The reactions were initiated by adding aliquots of the enzyme (0.16 μg for each test), and stopped at appropriate times with 4 ml of 1 M KOH. The released *p*-nitrophenol was determined by reading the absorbance at 400 nm (ε = 18,000 M^{-1} cm^{-1}). The main kinetic parameters (K_m and V_{max}) were determined by measuring the initial rates using eight different substrate concentrations in the 0.5–40 mM range. Experimental data were analyzed using the Michaelis-Menten equation and a nonlinear fitting program (FIGSYS).

To evaluate the inhibition power of compounds **4** and **16** we calculated the IC_{50} value using a fixed substrate concentration corresponding to the K_m of enzyme and varying inhibitor concentrations. The IC_{50} value was calculated by fitting experimental data with a non-nonlinear fitting program (FIGSYS, Biosoft, UK), using the equation:

$$Y = \frac{\text{Max} - \text{Min}}{1 + \left(\frac{x}{IC_{50}}\right)^{\text{slope}}} + \text{Min}$$

where '*y*' is vi/vo, that is, the ratio between the activity measure in the presence of the inhibitor (vi) and the activity of the control without the inhibitor (vo). The parameter '*x*' is the inhibitor concentration.

4.2.3. Animals

Male Wistar rats weighing 200–250 g bodyweight were housed at standard laboratory conditions and fed with a rodent pellet diet and water ad libitum. They were maintained at room temperature and at a photoperiod of 12 h day/night cycle. Animals described as fasted were deprived of food for 18 h but had free access to water. All animal procedures were conducted in accordance with our Federal Regulations for Animal Experimentation and Care (SAGARPA, NOM-062-ZOO-1999, México), and approved by the Institutional Animal Care and Use Committee based on US National Institute of Health publication (No. 85-23, revised 1985).

4.2.4. Induction of diabetes

Streptozotocin (STZ) was dissolved in citrate buffer (pH 4.5) and nicotinamide was dissolved in normal physiological saline solution. T2DM was induced in overnight fasted rats by a single intraperitoneal injection of 65 mg/kg streptozotocin, 15 min after the i.p. administration of 110 mg/kg of nicotinamide.[7,21] Hyperglycemia was confirmed by the elevated glucose concentration in plasma, determined at 72 h by glucometer. The animals with blood

glucose concentration higher 250 mg/dL, were used for the antidiabetic screening.

4.2.5. In vivo antidiabetic assay (T2DM model)[7]

The diabetic animals were divided into groups of five animals each ($n = 5$). Rats of experimental groups were administered a suspension of the compounds **1–7** (prepared in 1% Tween 80) orally (100 mg/kg body weight). Control group animals were also fed with 1% Tween 80. Glibenclamide (5 mg/kg) was used as hypoglycemic reference drug. Blood samples were collected from the caudal vein at 0, 1, 3, 5, and 7 h after vehicle, sample and drug administration. Blood glucose concentration was estimated by enzymatic glucose oxidase method using a commercial glucometer (Accutrend GCT, Roche®). The percentage variation of glycemia for each group was calculated in relation to initial (0 h) level, according to: %Variation of glycemia = $[(G_x - G_0)/G_0] \times 100$, where G_0 were initial glycemia values and G_x were the glycemia values at +1, +3, +5 and +7 h, respectively.[7] All values were expressed as mean ± S.E.M. Statistical significance was estimated by analysis of variance (ANOVA), $p < 0.05$ and $p < 0.01$ implies significance.

4.2.6. Docking

Molecular Operating Environment (MOE)[17] 2007 was used for ligand and protein preparation and molecular structure viewing. The crystal structure was obtained from the Protein Data Bank[22] with the accession code 2F71. Docking calculations were conducted with AUTODOCK 3.0.[16] In short, AUTODOCK performs an automated docking of the ligand with user-specified dihedral flexibility within a protein rigid binding site. The program performs several runs in each docking experiment. Each run provides one predicted binding mode. All water molecules, 1,2,3,4-tetrahydroisoquinolinyl sulfamic acid (crystallographic ligand), magnesium and chlorine ion, were removed from the Protein Data Bank file. Polar hydrogen atoms were added and Kollman charges,[23] atomic salvation parameters, and fragmental volumes were assigned to the protein. For validation of the docking protocol, ligand coordinates in the crystal complex were removed. For all ligands, Gasteiger charges[24] were assigned and non-polar hydrogen atoms were merged. All torsions were allowed to rotate during docking. The auxiliary program AutoGrid generated the grid maps. Each grid was centered at the crystallographic coordinates of the crystallographic sulfamic acid. The grid dimensions were $23 \times 23 \times 23$ Å^3 with points separated by 0.375 Å. Lennard-Jones parameters 12–10 and 12–6, supplied with the program, were used for modeling H-bonds and van der Waals interactions, respectively. The distance-dependent dielectric permittivity of Mehler and Solmajer[25] was used for calculation of the electrostatic grid maps. For all ligands, random starting positions, random orientations, and torsions were used. The translation, quaternion, and torsions steps were taken from default values in AUTODOCK. The Lamarckian genetic algorithm and the pseudo-Solis and Wets methods were applied for minimization using default parameters. The number of docking runs was 100. After docking, the 100 solutions were clustered into groups with RMS lower than 1.0 Å. The clusters were ranked by the lowest energy representative of each cluster. In order to describe the ligand-binding pocket interactions, the top ranked binding mode found by AUTODOCK in complex with the binding pocket of PTP-1B was subject to full energy minimization using the MMFF94 force field implemented in MOE until the gradient 0.05 was reached. During minimization, residue atoms within 8 Å from the ligand were free to move (other atoms were fixed).

Acknowledgments

This work was supported in part by grants from CONACYT, project 55591, given to G. Navarrete Vazquez. P. Paoli and G. Camici are grateful to the Italian MIUR for financial support (FIRB 2003-Project RBNE03FMCJ_007). H. Moreno-Diaz acknowledges the fellowships awarded by CONACyT to carry out graduate studies. J.L. Medina-Franco and K. Martínez-Mayorga are grateful to the State of Florida. Authors are grateful to AUTODOCK and VMD developers for providing the software.

References and notes

1. DeFronzo, R. A. *Diabetes Rev.* **1997**, *5*, 177.
2. Gallagher, E. J.; Leroith, D.; Karnieli, E. *Endocrinol. Metab. Clin. North Am.* **2008**, *37*, 559.
3. Hays, N. P.; Galassetti, P. R.; Coker, R. H. *Pharmacol. Ther.* **2008**, *118*, 181.
4. Sarabu, R.; Tilley, J. *Ann. Rep. Med. Chem.* **2005**, *40*, 167.
5. Elchebly, M.; Payette, P.; Michaliszyn, E.; Cromlish, W.; Collins, S.; Loy, A. L.; Normandin, D.; Cheng, A.; Himms-Hagen, J.; Chan, C. C.; Ramachandran, C.; Gresser, M. J.; Tremblay, M. L.; Kennedy, B. P. *Science* **1999**, *283*, 1544.
6. Seckl, J. R.; Walker, B. R. *Endocrinology* **2001**, *142*, 1371.
7. Moreno-Díaz, H.; Villalobos-Molina, R.; Ortiz-Andrade, R.; Díaz-Coutiño, D.; Medina-Franco, J. L.; Webster, S. P.; Binnie, M.; Estrada-Soto, S.; Ibarra-Barajas, M.; León-Rivera, I.; Navarrete-Vázquez, G. *Bioorg. Med. Chem. Lett.* **2008**, *18*, 2871.
8. Navarrete-Vázquez, G.; Moreno-Díaz, H.; Estrada-Soto, S.; Tlahuext, H. *Acta Crystallogr., Sect. E* **2008**, *64*, o608.
9. Stepanchikova, A. V.; Lagunin, A. A.; Filimonov, D. A.; Poroikov, V. V. *Curr. Med. Chem.* **2003**, *10*, 225.
10. Poroikov, V. V.; Filimonov, D. A.; Borodina, Y. V.; Lagunin, A. A.; Kos, A. *J. Chem. Inf. Comput. Sci.* **2000**, *40*, 1349.
11. Poroikov, V. V.; Filimonov, D. A. *J. Comput. Aided Mol. Des.* **2002**, *16*, 819.
12. Website: http://www.ibmh.msk.su/PASS.
13. Maccari, R.; Paoli, P.; Ottanà, R.; Jacomelli, M.; Ciurleo, R.; Manao, G.; Steindl, T.; Langer, T.; Vigorita, M. G.; Camici, G. *Bioorg. Med. Chem.* **2007**, *15*, 5137.
14. Wiesmann, C.; Barr, K. J.; Kung, J.; Zhu, J.; Erlanson, D. A.; Shen, W.; Fahr, B. J.; Zhong, M.; Taylor, L.; Randal, M.; McDowell, R. S.; Hansen, S. K. *Nat. Struct. Mol. Biol.* **2004**, *11*, 730.
15. Klopfenstein, S. R.; Evdokimov, A. G.; Colson, A. O.; Fairweather, N. T.; Neuman, J. J.; Maier, M. B.; Gray, J. L.; Gerwe, G. S.; Stake, G. E.; Howard, B. W.; Farmer, J. A.; Pokross, M. E.; Downs, T. R.; Kasibhatla, B.; Peters, K. G. *Bioorg. Med. Chem. Lett.* **2006**, *16*, 1574.
16. Morris, G. M.; Goodsell, D. S.; Halliday, R. S.; Huey, R.; Hart, W. E.; Belew, R. K.; Olson, A. J. *J. Comp. Chem.* **1998**, *19*, 1639.
17. Molecular Operating Environment (MOE) **2007**, Chemical Computing Group Inc., Montreal, Quebec, Canada. Available at: http://www.chemcomp.com.
18. Bialy, L.; Waldmann, H. *Angew. Chem., Int. Ed.* **2005**, *44*, 3814.
19. Zhang, S.; Zhang, Z. Y. *Drug Discovery Today* **2007**, *12*, 373.
20. Humphrey, W.; Dalke, A.; Schulten, K. *J. Mol. Graph.* **1996**, *14*, 33.
21. Masiello, P.; Broca, C.; Gross, R.; Roye, M.; Manteghetti, M.; Hillaire-Buys, D.; Novelli, M.; Ribes, G. *Diabetes* **1998**, *47*, 224.
22. Berman, H. M.; Westbrook, J.; Feng, Z.; Gilliland, G.; Bhat, T. N.; Weissig, H.; Shindyalov, I. N.; Bourne, P. E. *Nucleic Acids Res.* **2000**, *28*, 235.
23. Weiner, S. J.; Kollman, P. A.; Case, D. A.; Singh, U. C.; Ghio, C.; Alagona, G.; Profeta, S.; Weiner, P. A. *J. Am. Chem. Soc.* **1984**, *106*, 765.
24. Gasteiger, J.; Marsili, M. *Tetrahedron* **1980**, *36*, 3219.
25. Mehler, E. L.; Solmajer, T. *Protein Eng.* **1991**, *4*, 903.